J. Appl. Comput. Mech., 5(1) (2019) 162-173
DOI: 10.22055/JACM.2018.25857.1298

ISSN: 2383-4536
jacm.scu.ac.ir

M&MoCS
Shahid Chamran University of Ahvaz

Journal of
Applied and Computational Mechanics

Research Paper

Elastic-Plastic Analysis of Bending Moment – Axial Force Interaction in Metallic Beam of T-Section

M. Hosseini[1], H. Hatami[2]

[1] Department of Civil Engineering, Lorestan University, Khorram Abad, Iran
[2] Department of Mechanical Engineering, Lorestan University, Khorram Abad, Iran

Received May 15 2018; Revised June 22 2018; Accepted for publication June 24 2018.
Corresponding author: H. Hatami, hatami.h@lu.ac.ir

Abstract. This study derives kinematic admissible bending moment – axial force (M-P) interaction relations for mild steel by considering elastic-plastic idealizations. The interaction relations can predict strains, which is not possible in a rigid perfectly plastic idealization. The relations are obtained for all possible cases pertaining to the locations of neutral axis. One commercial rolled steel T-section is considered for studying the characteristics of interaction curves for different models. On the basis of these interaction curves, most significant cases for the position of neutral axis which are enough for the establishment of interaction relations are suggested.

Keywords: Elastic-Plastic Analysis; Mild Steel; T–Section; M-P interaction; Bending Moment.

1. Introduction

The study of structural failure under the impact loading is of importance for the safety and hazard assessment of structures. Simple structural elements like beams, plates, and shells fail in different modes under the dynamic loading. The beams being relatively critical elements have attracted more attention of scientists and engineers. The membrane force plays an important role in the dynamic response of a beam when the transverse deformations are sufficiently large, therefore, requiring axial force – bending moment interaction relations up to failure.

The standard static methods of analysis with dynamic magnification factors, for example, are not adequate in many dynamic plastic structural problems. Structural designers are often required to estimate the failure load of structural members for which they employ numerical techniques, such as the finite element method, but the analysis up to failure with large displacements and strains is usually difficult.

An early experimental study on the dynamic inelastic failure of beams was reported by Menkes and Opat who investigated the dynamic plastic response and failure of fully clamped metal beams which were subjected to uniformly distributed velocities over the entire span [1]. Menkes and Opat observed that the beams responded in a ductile manner and acquired permanently deformed profiles when subjected to velocities less than a certain value. However, when the impulsive velocities were equal to this critical value, then the beams failed owing to tearing of the beam material at the supports. As the impulsive velocities were further increased beyond this critical value, the failure occurred and the plastic deformation of the beams become more localized near the supports until another critical velocity, which was associated with a transverse shear failure at the supports, was reached [1].

The experimental results of Menkes and Opat were later analyzed by Jones using a simple rigid-plastic method [2]. A systematic study on the deformation and failure of fully clamped ductile beams struck by a mass was conducted by Liu and Jones [3, 4]. Two modes of failure – Tensile tearing and shear failure modes – were observed in experiments depending on the uniaxial rupture strain of the materials, the location of impact point, and support conditions [3]. The experiments on Aluminium beams showed that the geometry changes for the finite deflection play an important role in the dynamic response and the higher modal dynamic plastic response of the beams is more efficient in absorbing kinetic energy than the single modal response [5]. In a rigid-plastic structure, Shen and Jones assumed that the rupture occurs when the absorption of plastic work per unit volume reached a critical value [6]. To calculate the actual plastic work in beams, a hinge length was estimated from experimental data obtained by Menkes and Opat on impulsively loaded aluminium beams [1]. Continuum damage mechanics has been used recently for predicting the static and dynamic failure of beams [7, 8], but the method requires the values for several parameters, some of which are difficult to obtain.

The theoretical anomalous dynamic response of beams and a short pulse loading causing small deflections are studied by the elastic-plastic material model [9-11]. Another simpler and more attractive option for some problems is to carry out a rigid perfectly plastic analysis [12- 16] the accuracy of which is compared with the predictions of an elastic-plastic material [17- 22]. However, a rigid, perfectly plastic analysis does not predict strains so that it is difficult to study the failure unless some assumptions are made to overcome this difficulty.

In the present study, kinematic admissible interaction curves for the simultaneous action of bending moment and an axial force on a T-section are developed for elastic-plastic material idealizations. The interaction curves developed for T-section may be easily degenerated to the rectangular section. The procedure requires only the results from a standard uniaxial tensile test on the material.

Springback is one of the most common and important issues in the metal forming area. Due to the fact that springback depends on a variety of parameters, it is hard to predict. The effect of continuum damage mechanics (CDM) on the springback was investigated based on the Lemaitre isotropic unified damage law. The results indicated that considering the damage, the mechanics concept in springback modeling increases the predictability of the springback [23]. Khademalrsoul et al. investigated the implementations of different computational geometry technologies in the isogeometric analysis framework for computational fracture mechanics. Various numerical simulations demonstrated the suitability of the isogeometric approach in fracture mechanics [24]. Jinhai Zhao et al. investigated the similar new damage of fracture criteria to the local damage in conventional PD as the simulation fracture [25].

This study derives kinematic admissible bending moment – axial force (M-P) interaction relations for mild steel by considering elastic-plastic idealizations. One commercial rolled steel T-section is considered for studying the characteristics of interaction curves for different models. On the basis of these interaction curves, most significant cases for the position of the neutral axis which are enough for the establishment of interaction relations are suggested.

2. Stress-strain diagram

Direct tensile test results for a mild steel specimen ‘t036’ are taken as a reference for the modelling of stress-strain diagram (Table 1), which is thus idealized as linear for elastic strains followed by a flat yielding zone without strain hardening [8].

Table1. Static and dynamic tensile test for mild steel t036 [8]

σ_y (MPa)	σ_u (MPa)	E (GPa)	ν	ε_u
331	604	207	0.288	0.21

Therefore, the strain hardening is modelled by linear and parabolic models (Fig. 1). On the other hand, there are three zones in the idealized diagram: the elastic zone from $k = 0$ to $k = 1$; the yield zone without any strain-hardening from $k = 1$ to $k = k_1$; and the strain-hardening zone from $k = k_1$ to $k = k_2$, where $k\varepsilon_y$ is the strain. The stress in the strain-hardening range, σ_d at any strain, and $\varepsilon=k\varepsilon_y$ ($k_1<k<k_2$) can be obtained from the following relations [8]:

$$\sigma_d = \sigma_{yd} + \left(\sigma_{ud} - \sigma_{yd}\right) m \tag{1}$$

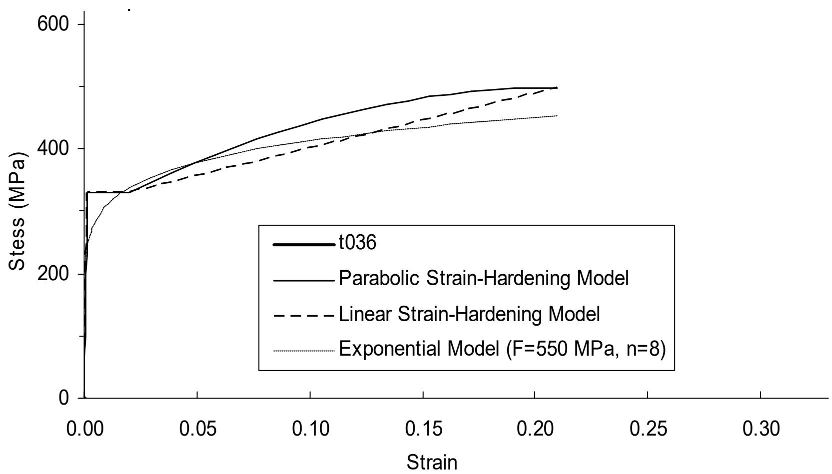

Fig. 1. Experimental stress-strain curve [8] and different models of mild steel

Equation 1 is for linear-hardening.

$$\sigma_d = \sigma_{yd} + \left(\sigma_{ud} - \sigma_{yd}\right)\left(2m - m^2\right) \tag{2}$$

Equation 2 is for parabolic-hardening.

$$m = \left(\frac{\varepsilon - \varepsilon_h}{\varepsilon_u - \varepsilon_h}\right) = \left(\frac{k - k_1}{k_2 - k_1}\right) \tag{3}$$

In Eq. 3, ε_h ($k_t\ \varepsilon_y$) is the strain corresponding to the initiation of strain hardening and ε_u ($k_2\ \varepsilon_y$) is the ultimate strain, σ_{yd} and σ_{ud} are the yield and ultimate dynamic stresses, respectively. The suffix d in the above-mentioned expressions is used to indicate dynamic values. The stress-strain curve can be used for the high strength steel by substituting K_1=1 and many other materials can be easily represented by these equations for different values of the parameters [8].

3. Bending moment axial force (M-P) interaction

Considering a T-section of beam with the width of flange, B, the thickness of flange, h, the overall depth, H, and the thickness of web, b, for studying the interaction of a bending moment, M, and an axial force, P (Fig. 2). The geometry of the section is defined by the following non-dimensional parameters:

$$\left.\begin{aligned} &\alpha = h / H \\ &\beta = \left(B - b\right)/B \\ &\gamma = b / B \\ &\gamma_1 = \alpha\beta\left(1-\alpha\right) \end{aligned}\right\} \tag{4}$$

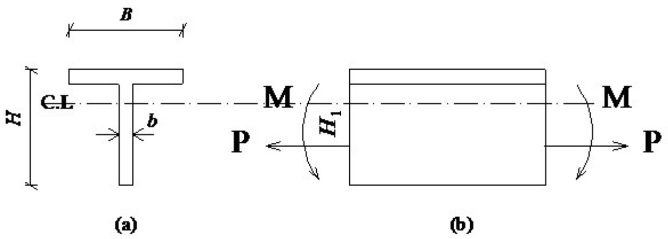

Fig. 2. (a) Section of beam, (b) An element subjected to external pull and bending moment

The T-section converts to the rectangular section when α=0 or 1, β=0, γ=1, γ_1=1. This Equation shows that the rectangular section has h=0 and H, therefore, $\alpha = h / H$ equals to 0 and 1. Moreover, in the rectangular section, the parameter β is 0 or B, therefore, $\beta = \left(B - b\right)/B$ equals to 1 or 0. The parameter γ can be 0 or B in the rectangular section, therefore, the parameter $\gamma = b / B$ can be 0 or 1.

The bending moment is assumed to cause compression at the top face. The axial force considered in the present analysis is tensile and the same relations can be used for a compressive axial force because the material behavior in compression is assumed to be the same as in tension. The interaction curves for different states of stresses are obtained in the subsequent subsections.

The extreme fiber strain in tension (i.e., at the bottom fiber) is taken as $k\varepsilon_y$ and the strain at the interface of the web with top flange is $k_t\varepsilon_y$. The extreme fiber strain at the top fiber is taken as $k'\varepsilon_y$ which is compressive when the neutral axis is inside the section, whereas it is tensile when the neutral axis is outside the section. The value of k' and k_t when the neutral axis lies inside the section are given by (Fig. 3) [12].

$$k' = k\frac{r}{1-r} \tag{5}$$

$$k_t = k\frac{r-\alpha}{1-r} \tag{6}$$

where $r = H_1/H_2$, H_1 = distance of the neutral axis from the extreme compression fiber. Moreover, when the neutral axis lies outside the section (Fig. 3), the value of k' and k_t are given by:

$$k' = k\frac{r}{1+r} \tag{7}$$

$$k_t = k\frac{r+\alpha}{1+r} \tag{8}$$

There are well-established interaction curves for elastic and a rigid perfectly plastic section having a rectangular cross-section, whereas for T-section these are derived in this section [12].

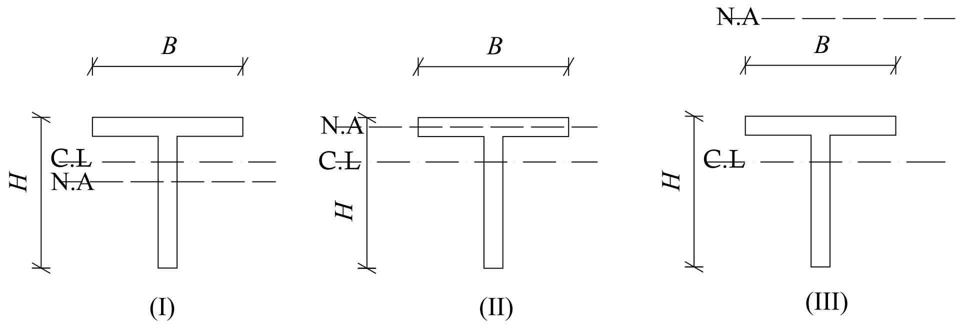

Fig. 3. Positions of neutral axis: (I) Neutral axis in web, (II) Neutral axis in flanges and (III) Neutral axis outside the section

4. Stress area

4.1 Elastic

4.1.1 Case-1 Neutral axis lies in the web i.e., 0< k '<1 (Fig. 4-a)

The M-P interaction relation obtained for this case is:

$$\bar{M} = \frac{2\alpha_1}{1-r}\left[\gamma(1-r)^3 + \beta(\alpha-r)^3 + r^3 - \frac{3}{2}\beta_1\bar{P}(\psi-2r)(1-r)\right] \tag{9}$$

$$r = \frac{\alpha^2\beta + \gamma - 2\beta_1\bar{P}}{2(\alpha\beta + \gamma - \beta_1\bar{P})} \tag{10a}$$

$$\alpha_1 = M_{1yd}/M_{yd} \tag{10b}$$

$$\beta_1 = P_{yd}/P_{1yd} \tag{10c}$$

$$P_{1yd} = \sigma_{yd}BH \tag{10d}$$

$$M_{1yd} = \sigma_{yd}BH^2/6, \quad \bar{P} = P/P_{yd} \tag{10e}$$

$$\psi = \frac{\alpha^2 + \gamma(1-\alpha^2)}{\alpha + \gamma(1-\alpha)} \tag{10f}$$

$$\bar{M} = \frac{M}{M_{yd}} \tag{10g}$$

$$P_{yd} = \sigma_{yd}\left[BH - (B-b)(H-h)\right] \tag{10h}$$

$$M_{yd} = \frac{\sigma_{yd}BH^2}{6\psi}\left\{\alpha^3\beta\left[1+3\left(\frac{\psi}{\alpha}-1\right)^2\right] + \gamma\left[1+3(1-\psi)^2\right]\right\} \tag{10i}$$

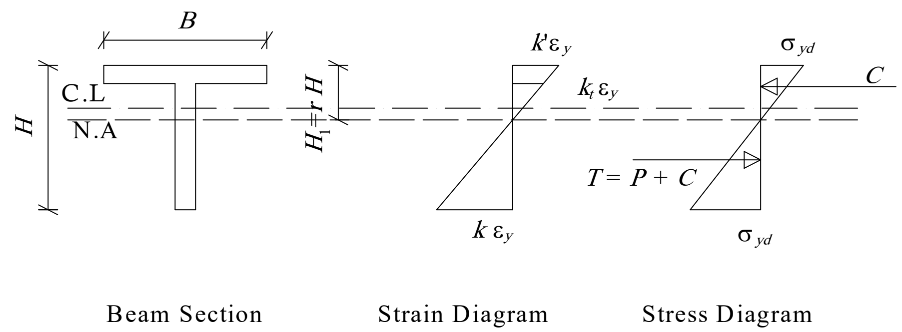

a)

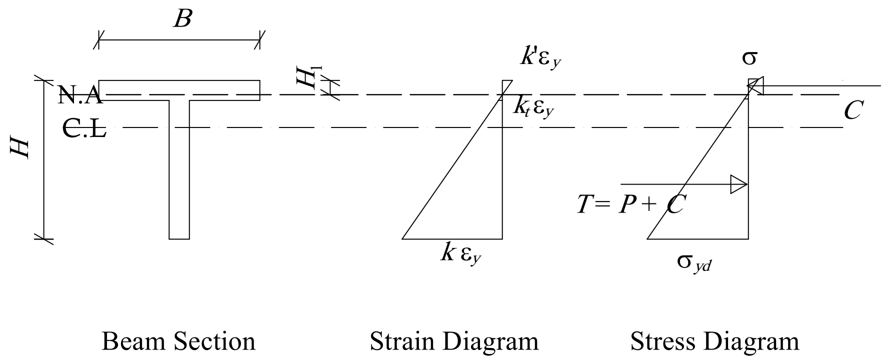

b)

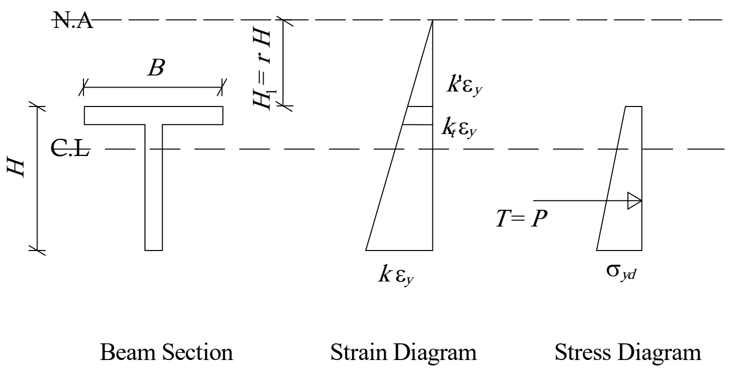

(c)

Fig. 4. Stress and strain variation in the section of a beam for different positions of neutral axis in the elastic model

Equation 9 converts to the rectangular section for α=0 or 1, β=0, γ =1, α_1=1, and β_1=0, therefore, it yields:

$$\psi = 1 \tag{11a}$$

$$M_{yd} = \frac{BH^2}{6} \tag{11b}$$

$$\overline{M} + \overline{P} = 1 \tag{11c}$$

4.1.2. Case-2 Neutral axis lies in the flange i.e., 0< k '<1 (Fig. 4-b)

The M-P interaction relation obtained for this case is:

$$\overline{M} = \frac{2\alpha_1}{1-r}\left[\gamma(1-r)^3 + \beta(\alpha - r)^3 + r^3 - \frac{3}{2}\beta_1\overline{P}(\psi - 2r)(1-r)\right] \tag{12}$$

The non-dimensional distance of the neutral axis, r, required for determining the value of k' from Eq. (5) may be obtained from the following equation:

$$r = \frac{\alpha^2\beta + \gamma - 2\beta_1\overline{P}}{2\left(\alpha\beta + \gamma - \beta_1\overline{P}\right)} \tag{13}$$

4.1.3. Case-3 Neutral axis is outside the section i.e., 0< k '<1 (Fig. 4-c)

The M-P interaction relation obtained for this case is:

$$\overline{M} = \frac{2\alpha_1}{1+r}\left[\gamma(1+r)^3 + \beta(\alpha + r)^3 - r^3 - \frac{3}{2}\beta_1\overline{P}(\psi + 2r)(1+r)\right] \tag{14}$$

The non-dimensional distance of the neutral axis, r, required for determining the value of k' from Eq. (7) may be obtained from the following equation:

$$r = -\frac{\alpha^2\beta + \gamma - 2\beta_1\overline{P}}{2\left(\alpha\beta + \gamma - \beta_1\overline{P}\right)} \tag{15}$$

In Fig. 7, the elastic case with black linear curve can be observed. The linear status can separate two part. One part for the force and another part for the moment. It can be seen that the force 0.6 with the moment 0.4 and the force 0.4 with the moment 0.6 too. Moreover, it can be seen that the sum of these two parts including the force 0.2 with the moment 0.8 and the force 0.8 with the moment 0.2 is always 1. Therefore, it can be used the superposition principle for the elastic case.

4.2. Plastic

For Rigid Perfectly Plastic case, there are two cases – one in which the neutral axis lies in the web and the other wherein neutral axis lies in the flange. These two cases are discussed in subsequent sub-sections.

4.2.1. Case-1 Neutral axis lies in the web i.e., $1< k' <k_l$ (Fig. 5-a)

The M-P interaction relation obtained for this case is:

$$\bar{M} = 3\alpha_1\left[\gamma(1-r)^2 - \beta(r-\alpha)^2 + r^2 - \beta_1\bar{P}(\psi - 2r)\right] \tag{16}$$

$$r = -\frac{\alpha\beta - \gamma + \beta_1\bar{P}}{2\gamma} \tag{17}$$

The above-mentioned equation converts to the rectangular section for α=0 or 1, β=0, γ=1, α_1=1, and β_1=0, therefore, it yields:

$$\frac{2}{3}\bar{M} + \bar{P}^2 = 1 \tag{18}$$

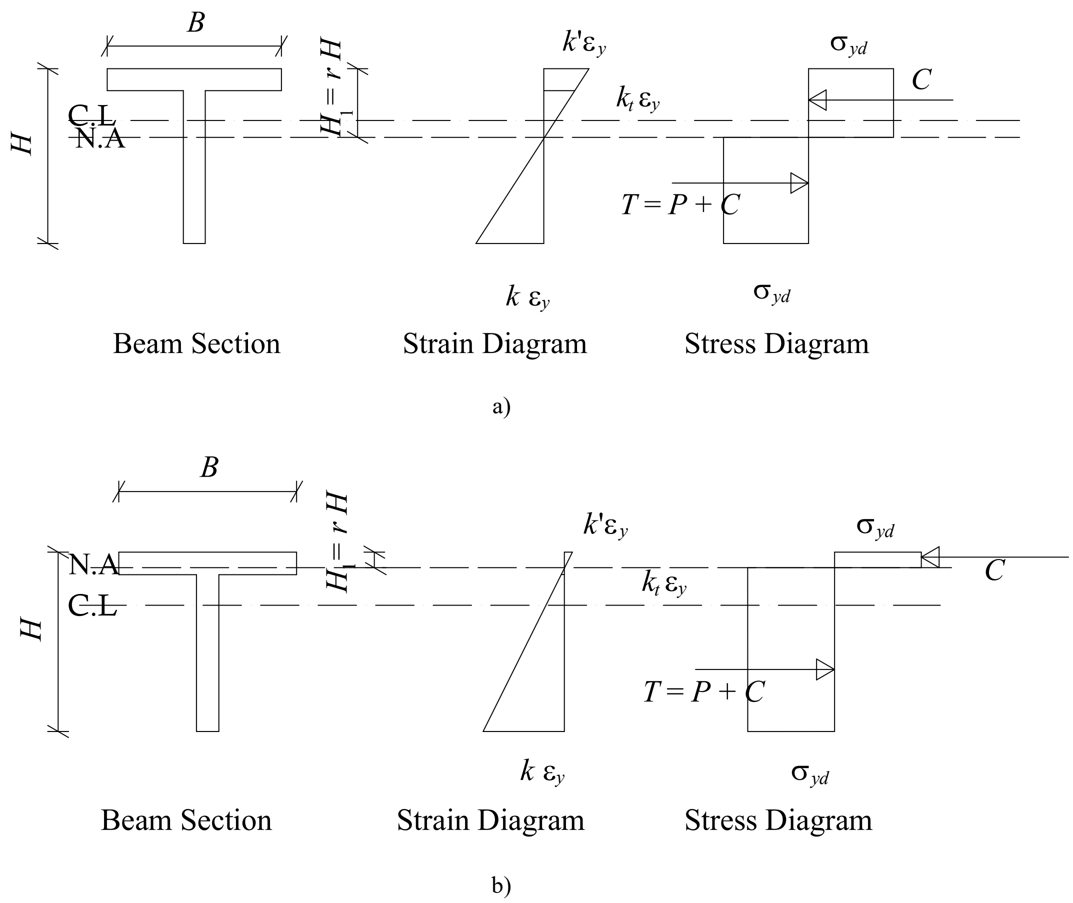

Fig. 5. Stress and strain variation in the section of a beam for different positions of neutral axis in the rigid perfectly plastic model

4.2.2. Case-2 Neutral axis lies inside the flange i.e., $1< k' <k1$ (Fig. 5-b)

The M-P interaction relation obtained for this case is:

$$\bar{M} = 3\alpha_1\left[\gamma(1-r)^2 + \beta(\alpha-r)^2 + r^2 - \beta_1\bar{P}(\psi - 2r)\right] \tag{19}$$

$$r = \frac{\alpha\beta + \gamma - \beta_1\bar{P}}{2} \tag{20}$$

The cross-section can only become fully plastic when the extreme fiber strain is infinite, which practically, it is not possible. The advantage of Eqs. 16 and 19 lies in their simplicity, but the main disadvantage is that it cannot predict strains. To overcome this difficulty, the elastic-plastic case is considered in the next subsection, which almost reduces to the rigid, perfectly plastic model for a large yield zone.

4.3 Elastic-plastic model

There are five cases for the elastic-plastic model of a T-section, which depend upon the position of the neutral axis. Three cases are associated with the neutral axis lying inside the cross-section and two cases lying outside the section (Fig. 6). The relations obtained for these cases are given below. The proof of Case–1 is given in Appendix A. Other expressions can be derived in a similar way.

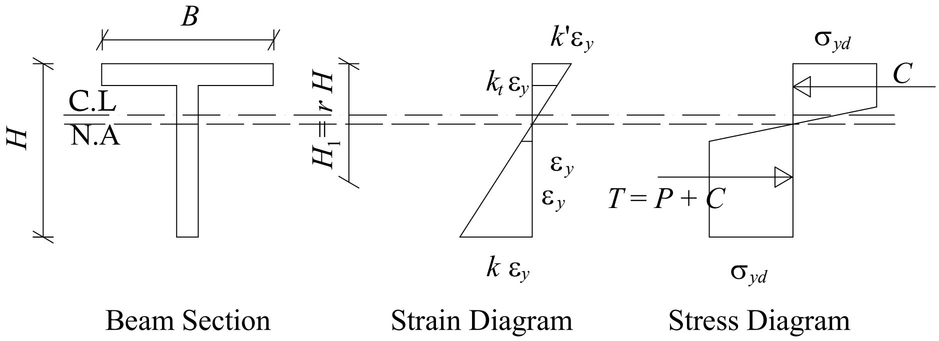

a)

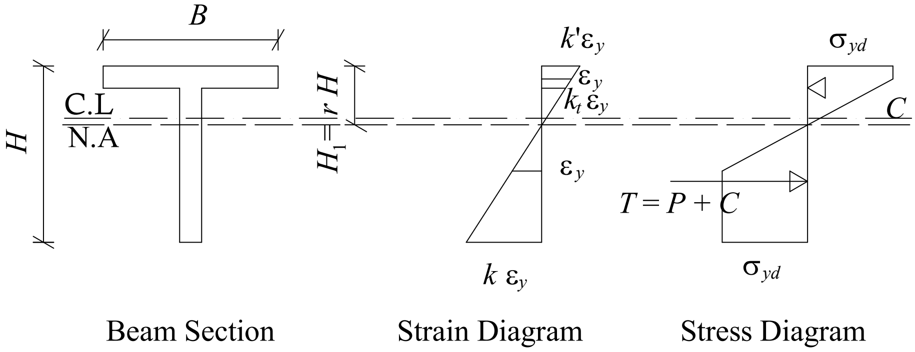

b)

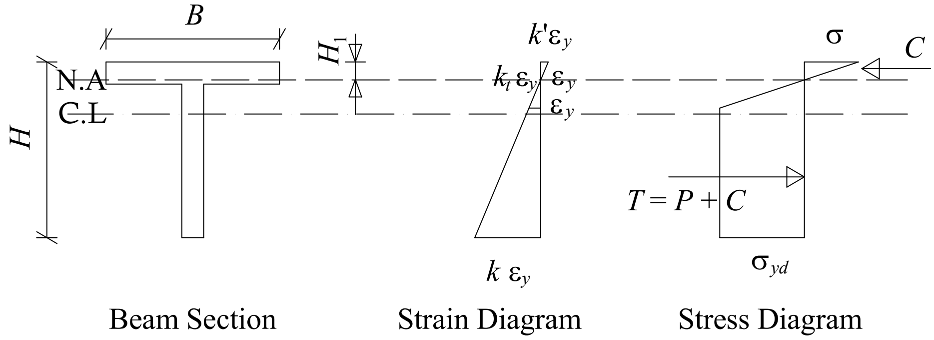

c)

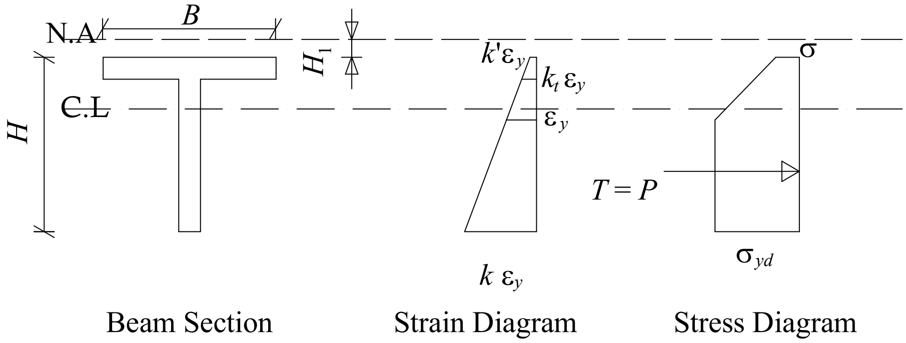

d)

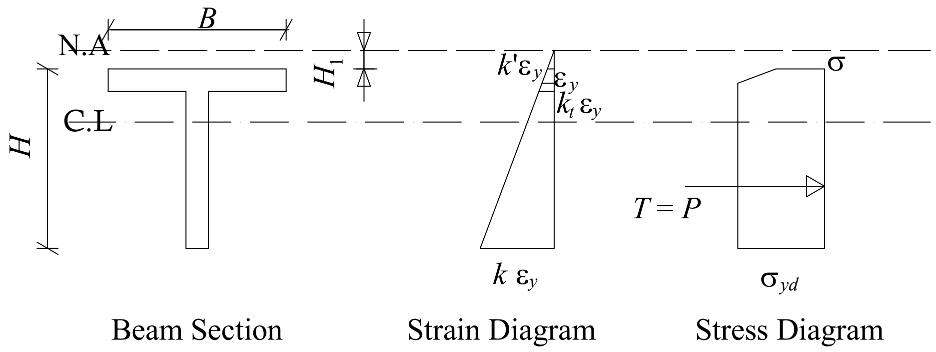

e)

Fig. 6. Stress and strain variation in the section of a beam for different positions of neutral axis in the elastic-plastic model

4.3.1 Case – 1: Neutral axis lies in the web i.e., $1< k' <k_1$ and $1<k_t$ (Fig.6-a)

The M-P interaction relation obtained for this case is:

$$\bar{M} = 3\alpha_1\left[\gamma r^2+\alpha\beta(2r-\alpha)+\gamma(1-r)^2\left(1-\frac{2}{3k^2}\right)+r^2-\beta_1\bar{P}(\psi-2r)\right] \tag{21}$$

The non-dimensional distance of the neutral axis, *r*, required for determining the value of k' from Eq. (5) may be obtained from the following quadratic equation:

$$r=\frac{1}{2\gamma}\left(-\alpha\beta+\gamma-\beta_1\bar{P}\right) \tag{22}$$

The proofs of Eqs. 21 and 22 are given in Appendix A. It can be seen from Eq.21 that for large values of the extreme fiber strain (i.e., k), the expression converts to Eq. 16. When there is no axial force (i.e., $\bar{P}=0$), the equation gives the maximum value of the shape factor for the elastic-plastic case as:

$$\bar{M} = 3\alpha_1\left[(1+\gamma)r^2+\alpha\beta(2r-\alpha)+\gamma(1-r)^2\left(1-\frac{2}{3k^2}\right)\right] \tag{23}$$

For a large value of k, the value of the shape factor given by the above-mentioned equation for wide T-sections of DIN CODE varies from 1.08 to 1.26, which is equal to the plastic shape factor of T-sections. The substitution of α=0 or 1, β=0, γ=1, α_1=1, and β_1=0 in the above-mentioned Eqs. 21 and 22 convert to the rectangular section as:

$$\bar{M}+\frac{1+3k^2}{2k^2}\bar{P}^2+\frac{\bar{P}}{k^2}=\frac{1-3k^2}{2k^2} \tag{24}$$

$$r=\frac{1}{2}\left(1-\bar{P}\right) \tag{25}$$

4.3.2 Case – 2: Neutral axis lies in the web i.e., $1<k'<k_1$ and $0<k_t<1$ (Fig. 6-b)

The M-P interaction relation obtained for this case is:

$$\bar{M} = \alpha_1\left[3r^2-\left(\frac{r}{k'}\right)^2\left\{1+\gamma-3\gamma k^2-2\beta k_t^3\right\}-3(1-2r)\beta_1\bar{P}\right] \tag{26}$$

The non-dimensional distance of the neutral axis, *r*, required in the above-mentioned equation and also for determining the value of k' from Eq. 5 may be obtained from the following quadratic equation:

$$\left[2\gamma+\frac{\beta}{2k}(1+k)^2\right]r^2-\left[1+2\gamma+\frac{\beta}{k}\left(1+\alpha k^2\right)-\beta_1\bar{P}\right]r+\left[\gamma+\frac{\beta}{2k}+\frac{k\alpha^2\beta}{2}-\beta_1\bar{P}\right]=0 \tag{27}$$

4.3.3 Case – 3: Neutral axis lies in the flange i.e., $0< k' <1$ and $0<k_t<1$ (Fig. 6-c)

The M-P interaction relation obtained for this case is:

$$\bar{M} = \alpha_1\left[2k'r^2+\left(\frac{r}{k'}\right)^2\left\{3\gamma k^2+2\beta k_t^3-\gamma\right\}-3(1-2r)\beta_1\bar{P}\right] \tag{28}$$

The non-dimensional distance of the neutral axis, *r*, required in the above-mentioned equation and also for determining the value of k' from Eq. 5 may be obtained from the following quadratic equation:

$$\gamma\left[\left(1-\frac{1}{2k}\right)-\frac{k}{2}\right]r^2-\left[\alpha\beta k+\gamma\left(2-\frac{1}{k}\right)-\beta_1\bar{P}\right]r+\left[\frac{k\alpha^2\beta}{2}+\gamma\left(1-\frac{1}{2k}\right)-\beta_1\bar{P}\right]=0 \tag{29}$$

4.3.4 Case – 4: Neutral axis outside the section and 0< k' <1 and 0< k_t <1 (Fig. 6-d)

The M-P interaction relation obtained for this case is:

$$\bar{M}=3\alpha_1\left[\gamma(1+2r)-\alpha\beta\left(k_t-k'\right)(\alpha+3r)+\alpha\beta k_t(\alpha+2r)-\frac{\gamma}{3}\left(\frac{r}{k'}\right)^2\left(1-k'\right)^2\left(1+2k'\right)-(1+2r)\beta_1\bar{P}\right] \tag{30}$$

The non-dimensional distance of the neutral axis, *r*, required in the above-mentioned equation and for determining the value of k' from Eq. 7 may be obtained from the following quadratic equation:

$$\left[-\gamma\frac{(1-k)^2}{2k}\right]r^2+\left[\alpha\beta k+2\gamma-\frac{\gamma}{k}-\beta_1\bar{P}\right]r+\left[\frac{k\alpha^2\beta}{2}+\gamma\left(1-\frac{1}{2k}\right)-\beta_1\bar{P}\right]=0 \tag{31}$$

4.3.5. Case – 5: Neutral axis outside the section and 0<k'<1 and 0< k_t <1 (Fig. 6-e)

The M-P interaction relation obtained for this case is:

$$\bar{M}=3\alpha_1\left[\gamma(1+2r)+\alpha\beta(\alpha+2R)-\frac{1}{3}\left(\frac{r}{k'}\right)^2\left(1-k'\right)^2\left(1+2k'\right)-(1+2r)\beta_1\bar{P}\right] \tag{32}$$

The non-dimensional distance of the neutral axis, *r*, required in the above-mentioned equation and also for determining the value of k' from Eq. (7) may be obtained from the following quadratic equation:

$$-\frac{(1-k)^2}{2k}r^2+\left[\alpha\beta+\gamma-\frac{1-k}{k}-\beta_1\bar{P}\right]r+\left[\alpha\beta+\gamma-\frac{1}{2k}-\beta_1\bar{P}\right]=0 \tag{33}$$

One T-section, T100*100*10 of DIN code, is taken for the numerical study. The M-P interaction curve considering all these five cases is plotted for the T-section taking different values of *k* (Fig. 7). It can be seen from these figures that the curve approaches the rigid perfectly plastic case for large values of *k* ($k \geq 10$), as required by the limit theorems of plasticity [12].
For these equations, the parameters k, α, β, γ are replacing numerically (for example: 0< k' <1 and 0< k_t <1 , $\alpha=0{,}1$, $\beta=0{,}1$, and $\gamma=0{,}1$) and then these equations are solved using numerical method because they have many different parameters and there are two equations (32 and 33).

5. Discussion

One quadrant of the M-P interaction curves for the T-section is plotted for the elastic-plastic models (Fig. 7). The M-P interaction curves for all the models are plotted (Fig. 8). The observations made from these figures are as follows:

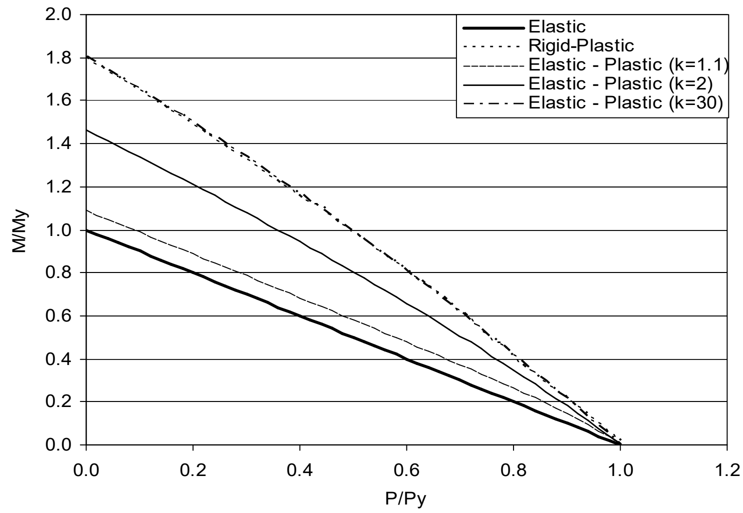

Fig. 7. M-P interaction curves for elastic, plastic and elastic-plastic models for T-section (T100*100*10)

- The elastic-plastic interaction curve for $k=k_1$ is close to the rigid perfectly plastic curve for large values of the yield strains (k_1>10) for of the T-section. There are five parts in the elastic-plastic curve arising due to the five positions of the neutral axis (Fig. 6). The fourth case, i.e., with the neutral axis outside the section and k_t<1, represents a small zone of the interaction curve for large values of k1 (say, k_1>10). The result of elastic-plastic interaction curve for five parts are shown in Fig. 6. For example, for the case 1 in 5 parts, the strain diagram has negative and positive strain and the limit of positive strain is $k'\varepsilon_y$ and in negative limit of strain is $k\varepsilon_y$. In part 3, the smaller positive limit and larger negative limit are observed. At least in part 5, the zero positive strain and largest negative strain $k\varepsilon_y$ can be observed. When the neutral axis is out of section state, $k'\varepsilon_y = 0$ is observed (Fig. 6).

- Only five cases, 1, 2, 3, 4, and 5 (first five for the neutral axis inside the section), are sufficient for practical purposes for defining the interaction curve of mild steel T-sections. All the five possible cases are required to define the interaction curve for an elastic-plastic material.
- The strains and hence the strain rates due to bending and an axial force can be separated only for the linear-elastic case because the principle of superposition is not valid for the nonlinear case.
- The M-P interaction curves for elastic-plastic are non-convex for large values of the axial force when the neutral axis lies outside the section and are convex when the neutral axis lies inside the section.

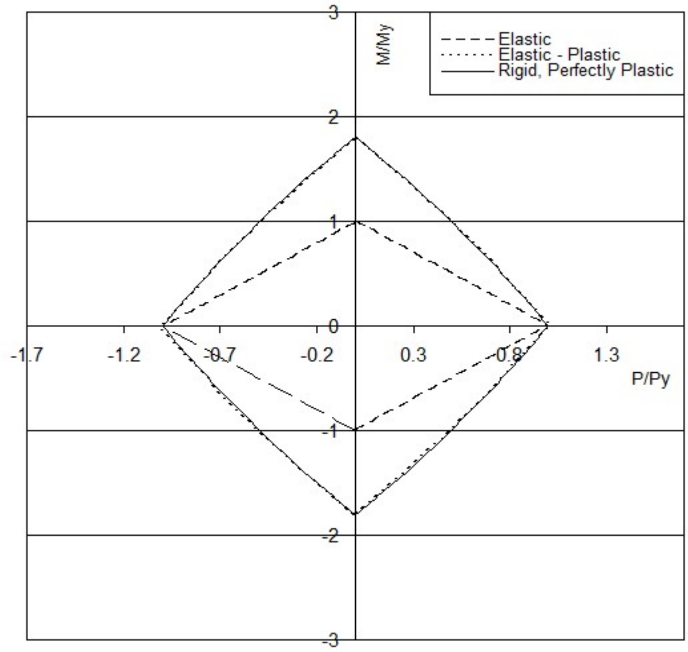

Fig. 8. M-P interaction curves for different models (k=k_1=12 for elastic-plastic and k=k_l=127 for linear and parabolic hardening curves) for T-section (T100*100*10)

6. Conclusion

The M-P (Bending Moment – Axial Force) interaction curves are developed for T-section with elastic-plastic idealizations of the mild steel. The M-P interaction relations are expressed in terms of the extreme fiber strains, which is not possible for a rigid perfectly plastic model. The relations are obtained for different practically possible cases related to different locations of the neutral axis. These relations easily degenerate to the rectangular section by some simple substitutions. The interaction curves of the rectangular section can be obtained by some simple substitutions. One T-section, T100*100*10, is considered for studying the characteristics of interaction curves. The conclusions derived from this numerical study are as follows:

- The elastic-plastic interaction curve approaches the rigid perfectly plastic curve for large values of the yield strains for one of the T-sections. There are five parts in the elastic-plastic curve arising due to the five positions of the neutral axis. The fourth case, i.e., with the neutral axis outside the section and the strain in the extreme top fiber is less than the yield strain, represents a small zone of the interaction curve for large values of yield strain coefficient, k_1 (say, k_1>10).
- Though there are many possible cases related to different locations of neutral axis, but the portion of the interaction curve represented by many of these cases is very small and could be ignored. It is found that only five cases, four for the neutral axis inside the section and one for the neutral axis outside the section (Cases 1-5, 8, & 11), are sufficient for practical purposes for defining the interaction curve of mild steel T-section.
- The strains and hence the strain rates due to bending and an axial force can be separated only for the linear-elastic case because the principle of superposition is not valid for the nonlinear case.

Though the above-mentioned conclusions are derived for the one typical T-section considered in the study, but other T-sections being similar. The above-mentioned conclusions may be considered to be general for any T-sections.

Conflict of Interest

The authors declare no conflict of interest.

Nomenclature

B	Width of beam	R	Radius of curvature
b	Thickness of web of the beam	$\alpha\,\beta\,\gamma$	Parameters
H	Depth of beam	$\alpha_1\,\beta_1\,\gamma_1$	Parameters
h	Thickness of flange	ε	Normal strain
H_1	Distance of neutral axis (N.A.) from extreme compression fiber	ε_y	Yield strain
E	Modulus of elasticity	$\varepsilon_m = k\,\varepsilon_y$	Strain in extreme fiber
r	Non-dimensional distance of neutral axis from extreme compression fiber $= H_1 / H$	$\varepsilon_h = k_1 \varepsilon_y$	Strain corresponding to end of yielding and beginning of strain-hardening
m	Parameter	$\varepsilon_u = k_2 \varepsilon_y$	Ultimate strain
M	Bending moment at the section	σ	Normal stress
M_{yd}	Dynamic yield moment for T-section	σ_{yd}	Dynamic yield stress
M_{1yd}	Dynamic yield moment for rectangular section = $\sigma_{yd} BH^2 / 6$	σ_{ud}	Dynamic ultimate stress
$\overline{M}$	$\dfrac{M}{M_{yd}}$ = shape factor of T-section when yield stress is σ_{yd}	d	Dynamic
P	Axial force on the section	h	Beginning of hardening
P_{yd}	Yield force for T-section = $\sigma_{yd}\left[BH - (B-b)(H-h)\right]$	t	top
P_{1yd}	Yield force for rectangular section = $\sigma_{yd} BH$	u	Ultimate
$\overline{P}$	P / P_{yd}	y	Yield

References

[1] S.B. Menkes, H.J. Opat., Broken beams, *Exp Mech*, 13 (1973) 480-486.

[2] N. Jones., Plastic failure of ductile beams loaded dynamically, Trans. *ASME. J Eng Ind*, 98 (1976) 131-136.

[3] J.H. Liu, N. Jones., Experimental investigation of clamped beams struck transversely by a mass, *Int J Impact Eng*, 6 (1987) 303-335.

[4] J.H. Liu, N. Jones, Plastic failure of a clamped beams struck transversely by a mass, University of Liverpool, Department of Mechanical Engineering Report ES/13/87, presented at A. Sawczuk Memorial Syp. Rytto Poland. To be published by pineridge Press, Swansea 1988.

[5] N. Jones, C.G. Soares, Higher Model Dynamic, Plastic Behavior of Beam Loaded Impulsively, *Int Mech. Sci*, 20 (1977) 135-147.

[6] W.Q. Shen, N. Jones, A failure criterion for beams under impulsive loading, *Int J Impact Eng*, 12 (1992) 101-121.

[7] M. Alves, N. Jones, Impact failure of beams using damage mechanics: Part I – Analytical model, *Int J Impact Eng*, 27 (2002) 837-861.

[8] M. Alves, N. Jones, Impact failure of beams using damage mechanics: Part II – Application, *Int J Impact Eng*, 27 (2002) 863-890.

[9] P.S. Symonds, F. Genna, A. Ciullini, Special cases in study of anomalous dynamic elastic-plastic response of beams by a simple model, *Int J Solids Structures*, 27 (1991) 299-314.

[10] Y. Qian, P.S. Symonds, Anomalous dynamic elastic-plastic response of a Galerkin beam model, *Int J Mech Sci*, 38 (1996) 687-708.

[11] A. Bassi, F. Genna, P.S Symonds, Anomalous elastic-plastic responses to short pulse loading of circular plates, *Int J Impact Eng*, 28 (2003) 65-91.

[12] N. Jones, Structural Impact, Cambridge: Cambridge University Press, 1989, Paperback edition, 1997.

[13] Q.M. Li, Continuity conditions at bending and shearing interfaces of rigid, perfectly plastic structural elements, *Int. J. Solid and Struc.*, 37 (2000) 3651-3665.

[14] M. Ostoja-Starzewski, H. Ilies, The Cauchy and characteristic boundary value problems of random rigid-perfectly plastic media, *Int. J. solids and Struc.*, 33 (1996) 1119-1136.

[15] C.A. Anderson, R.T. Shield, A class of complete solutions for bending of perfectly-plastic beams, *Int. J. Solids and Struc.*, 3 (1967) 935-950.

[16] Q. Zhou, T.X. Yu, H. Zhuping, The large deflection of a rigid-perfectly plastic portal frame subjected to impulsive loading, *Int. J. Solids and Struc.*, 26 (1990) 1225-1242.

[17] M.R. Brake, An analytical elastic-perfectly plastic contact model, *Int. J. Solids and Struc.*, 49 (2012) 3129-3141.

[18] Y.T. Cheng, Ch.M. Cheng., Scaling relationships in conical indentation of elastic-perfectly plastic solids, *Int. J. Solids and Struc.*, 36 (1999) 1231-1243.

[19] P.N. Zouain, L.A. Borges, M.B. Hecke. A force method for elastic-plastic analysis of frames by quadratic optimization, *Int. J. solids and Struc.*, 24 (1988) 211-230.

[20] P.S. Symonds, C.W.G. Frye, On the relation between rigid-plastic and elastic-plastic predictions of response to pulse loading, *Int. J. Impact Eng.*, 7 (1988) 139-149.

[21] T.X. Yu, Elastic effects in the dynamic plastic response of structures, In: N. Jones, T. Wierzbicki, editors. Structural crashworthiness and failure, Elsevier Applied Science, London and New York, 1993, 341-384.
[22] M. Hosseini, H. Abbas, Strain hardening in M–P interaction for metallic beam of I-section, *Thin-Walled Structures*, 62 (2013) 243–256.
[23] M. Shahabi, A. Nayebi, Springback Modeling in L-bending Process Using Continuum Damage Mechanics Concept, *Journal of Applied and Computational Mechanics*, 1(3) (2015) 161-167.
[24] A. Khademalrsoul, R. Naderi, Local and Global Approaches to Fracture Mechanics Using Isogeometric Analysis Method, *Journal of Applied and Computational Mechanics*, 1(4) (2015) 168-180.
[25] J. Zhao, H. Tang, S. Xue, Modelling of crack growth using a new fracture criteria based peridynamics, *Journal of Applied and Computational Mechanics*, 2018, DOI: 10.22055/JACM.2017.23515.1160.

APPENDIX – A

Mathematical Proofs

Elastic-Plastic (Case – I)

The total compressive force on the section can be obtained by integrating the stresses over the section in compression, thus it yields (Fig. 6-a)

$$C = \sigma_{yd}\left[h\left(B-b\right)+bH_1-b\frac{H-H_1}{2k}\right]=P_{1yd}\left[\alpha\beta+\gamma r\left(1-\frac{1}{2k'}\right)\right] \tag{A.1}$$

Similarly, the total tensile force is (Fig. 6-a)

$$T = \sigma_{yd}\left[b\left(H-H_1\right)-b\frac{H-H_1}{2k}\right]=P_{1yd}\left[\gamma\left(1-r\right)\left(1-\frac{1}{2k}\right)\right] \tag{A.2}$$

The distance of the line action of the resultant compressive and tensile forces from the neutral axis can be found by taking the moment of the different force components, thus it yields:

$$\bar{y}_C = \frac{3M_{1yd}}{C}\left[\alpha\beta\left(2r-\alpha\right)+\gamma r^2\left\{1-\frac{1}{3\left(k'\right)^2}\right\}\right] \tag{A.3}$$

$$\bar{y}_T = \frac{3M_{1yd}}{T}\left[\gamma\left(\frac{r}{k'}\right)^2\left(k^2-\frac{1}{3}\right)\right] \tag{A.4}$$

The position of the neutral axis can be found by considering the equilibrium of forces,

$$P = T - C \tag{A.5}$$

Which using Eqs. (A.1) and (A.2) gives

$$P = \sigma_{yd} b\left(H-2H_1\right)=P_{1yd}\left(\gamma-2\gamma r-\alpha\beta\right) \tag{A.6}$$

from which the position of neutral axis is

$$r = \frac{1}{2\gamma}\left(-\alpha\beta+\gamma-\beta_1\bar{P}\right) \tag{A.7}$$

which is the same as Eq. (22) in this study. The moment of bending resistance of the section is

$$M = C\bar{y}_C + T\bar{y}_T - P\left(\frac{H}{2}\psi-H_1\right) \tag{A.8}$$

or

$$\overline{M} = \frac{C\,\overline{y}_C}{M_{yd}}+\frac{T\,\overline{y}_T}{M_{yd}}-\frac{PH}{2M_{yd}}\left(\psi-2r\right) \tag{A.9}$$

or

$$\bar{M} = 3\alpha_1\left[\gamma r^2+\alpha\beta\left(2r-\alpha\right)+\gamma\left(1-r\right)^2\left(1-\frac{2}{3k^2}\right)+r^2-\beta_1\bar{P}\left(\psi-2r\right)\right] \tag{A.10}$$

which is the same as Eq. (21) in this study.